

# Through-Space Spin–Spin Coupling in van der Waals Dimers and CH/ $\pi$ Interacting Systems. An Ab Initio and DFT Study

Alessandro Bagno,\* Giacomo Saielli, and Gianfranco Scorrano<sup>[a]</sup>

**Abstract:** The through-space  $J_{\text{HH}}$  and  $J_{\text{CH}}$  spin–spin coupling constants of model van der Waals dimers (involving methane, ethylene, and benzene), and of selected compounds showing the CH/ $\pi$  interaction, have been investigated by means of DFT and ab initio calculations. In the range of intermolecular separations for which the interaction is stabilizing, weak couplings (0.1–0.3 Hz) are predicted for  $J_{\text{CH}}$ , while the corresponding  $J_{\text{HH}}$  couplings are much smaller. The

relative contributions (Fermi-contact, spin–orbit, and spin–dipole) are strongly dependent on the geometry of the dimers and on the distance; the non-negligible values of  $J_{\text{CH}}$  for  $\pi$  systems

**Keywords:** ab initio calculations • CH/ $\pi$  interactions • density functional calculations • NMR spectroscopy • spin–spin coupling • van der Waals interactions

stem largely from an incomplete cancellation of spin–orbit terms. The results obtained for the larger molecules, that is, acetonitrile@calix[4]arene **5**, the imine **6**, and the aryl ester **7** are consistent with those on the model dimers. For **7**, the occurrence of a through-space mechanism for the transmission of coupling is established by examining trends in the magnitude of couplings as a function of the number of intervening covalent bonds.

## Introduction

Spin–spin (scalar)  $J$ -coupling is normally thought of as a probe of connectivities through covalent bonds only. As such, in NMR spectroscopy it is employed in a variety of experiments to elucidate the general molecular framework, as well as conformational problems involving covalently bonded groups. Recently, it has been demonstrated that spin–spin coupling can also be transmitted through hydrogen bonds (HB), as long as the two interacting moieties remain at a suitable distance for a time long enough for NMR detection. This appears to be the case for several proteins,<sup>[1–3]</sup> DNA and RNA base pairs,<sup>[1, 4]</sup> phosphorus compounds,<sup>[5]</sup> and HF complexes at low temperature;<sup>[1, 6]</sup> such through-HB coupling constants involving  $^1\text{H}$ ,  $^{13}\text{C}$ ,  $^{15}\text{N}$ , or  $^{31}\text{P}$  lie between 0.1 and 7 Hz, but are much larger for couplings involving  $^{19}\text{F}$  in  $(\text{HF})_n \cdots \text{F}^-$  complexes.<sup>[6]</sup> Most notably, state-of-the-art NMR techniques have made it possible to detect coupling constants as small as 0.14 Hz.<sup>[3]</sup>

These findings have stimulated much theoretical work aimed at a better understanding of the underlying factors, like the influence of the distance, orientation, and HB type on the coupling constant.<sup>[1, 7–15]</sup> Barfield et al. recently studied the  $^2J_{\text{NN}}$  ( $^{15}\text{N}–\text{H} \cdots ^{15}\text{N}$ ) of DNA triplets,<sup>[9]</sup> Scheurer et al.<sup>[10]</sup> and

Pecul et al.,<sup>[14]</sup> as well as our group<sup>[15]</sup> have analyzed the through-HB coupling constant  $^3J_{\text{NC}}$  ( $^{15}\text{N}–\text{H} \cdots \text{O}=\text{C}$ ) in amide HB dimers as a function of the HB structure; this led to predicted values lying in the correct range of the available experimental results. These observations have an obvious bearing on the hypothetical covalent character of the HB.<sup>[16, 17]</sup>

The connection between HB type, strength, and NMR properties (including spin–spin coupling) has been investigated by Del Bene and Bartlett.<sup>[11–13]</sup>

The unusually large long-range  $J$  couplings involving  $^{19}\text{F}$  have been known for quite some time, and a through-space mechanism has been invoked in this connection, for example to explain  $^6J_{\text{HF}}$  and  $^5J_{\text{CF}}$  couplings in fluoronaphthalenes.<sup>[18]</sup> Recently, Oldfield and co-workers demonstrated the through-space nature of  $J_{\text{FF}}$  spin–spin couplings in fluoronaphthalenes by DFT methods.<sup>[19]</sup>

It is worthwhile to note that, despite the fact that the term “through-space” is now commonly used in the literature (and we will conform to this usage), this should not be meant as implying a different physical origin. In fact, the mechanisms responsible for these couplings are exactly the same as for covalently and hydrogen-bonded nuclei.

An obvious extension of the above ideas is that spin–spin coupling might be detectable even in the case of dispersion-bound van der Waals complexes. In fact, Salsbury and Harris calculated finite but very small ( $<10^{-3}$  Hz) couplings for  $\text{Xe} \cdots \text{Xe}$  and  $\text{Xe} \cdots \text{H}$ .<sup>[20]</sup> More interestingly, Pecul et al. calculated a surprisingly large coupling for the helium dimer<sup>[21a]</sup> ( $J_{\text{He},^3\text{He}} = 1.3$  Hz at the equilibrium distance) and the  $\text{HF} \cdots \text{CH}_4$  van der Waals dimer ( $J_{\text{HF}} = \text{ca. } 4$  Hz).<sup>[21b]</sup>

[a] Dr. A. Bagno, Dr. G. Saielli, Prof. G. Scorrano  
Centro CNR Meccanismi Reazioni Organiche  
Dipartimento di Chimica Organica, Università degli Studi di Padova  
Via Marzolo 1, 35131, Padova (Italy)  
Fax: (+39) 049-827-5239  
E-mail: alessandro.bagno@unipd.it

Although the existence of scalar coupling between “unbound” nuclei has obvious fundamental implications, the experimental verification will be fraught with very great difficulties, both owing to their small magnitude and, especially, to the probable floppiness of these weakly bound systems, which might be in the fast-exchange regime between “bound” and “unbound” states on the NMR time scale (except, perhaps, at extremely low temperatures). Nevertheless, exploiting couplings to  $^{129}\text{Xe}$  might be important in relation to the use of optically pumped xenon as a spin probe in host–guest complexes.<sup>[22]</sup>

There is, moreover, a very broad range of organic host–guest complexes, which often owe their stability and structure to favorable dispersive interactions, as well as flexible molecules that exhibit folded conformers stabilized in this way. In such cases, the importance of the CH/ $\pi$  interaction as a factor to stabilize such host–guest complexes, or the folded conformer, has been widely recognized.<sup>[23]</sup> In a recent work, Takahashi et al.<sup>[24]</sup> examined the structure of several host–guest compounds deposited in the Cambridge Crystallographic Database<sup>[25]</sup> in order to understand the relevance of the CH/ $\pi$  interaction in the stabilization of the complexes. In a large number of cases, short distances between a hydrogen of the host (guest) compound and an aromatic portion of the guest (host) compound have been found—often as short as 2.7 Å for both alkyl and aromatic C–H bonds. Short distances between a hydrogen and a  $\pi$  system have also been observed in several cases of intramolecular CH/ $\pi$  interaction.<sup>[23]</sup> Owing to the relatively close contact of the atoms involved, these cases represent the best examples of systems in which through-space spin–spin coupling may be detectable; in fact, a through-space  $^1\text{H}$ ,  $^{203,205}\text{Tl}$  coupling of 17 Hz has been experimentally determined for a dithallium cryptate.<sup>[26]</sup>

These circumstances prompted us to investigate the intermolecular spin–spin coupling in model complexes structur-

ally related to the above systems. Indeed, by means of DFT calculations we predicted that, at least for two simple van der Waals dimers (methane–benzene and benzene–benzene), a small but non-negligible  $^{13}\text{C}$ ,  $^1\text{H}$  coupling (0.2–0.3 Hz) may exist between nuclei belonging to nonbonded molecules.<sup>[27]</sup>

Herein we wish to broaden the scope of this investigation to other van der Waals dimers involving methane, ethylene, and benzene (Figure 1), including **3b** and **4b**, which have already been presented.<sup>[27]</sup> For the smaller dimers we also compare DFT results with those from ab initio methods currently in use for such calculations. Based on the results obtained from the model systems, we also extend our investigation to a few compounds for which through-space spin–spin coupling is expected to occur because of the similar structural arrangements. These are the inclusion compound acetonitrile@calix[4]arene **5**, the imine **6**, and the aryl ester **7**, reported in Figure 2.

## Computational Methods

**Energetics:** The stabilization energy for the various dimers was calculated by using *Gaussian 98*.<sup>[28]</sup> Interaction energies were counterpoise corrected<sup>[29]</sup> for the basis set superposition error (BSSE). The stabilization energy of van der Waals complexes is entirely due to the dispersive interaction, which in turn is due to electron correlation. Second-order Møller–Plesset theory (MP2) was employed for this purpose, since higher-order levels are too computationally demanding for a systematic investigation of relatively large dimers like  $\text{C}_6\text{H}_6 \cdots \text{C}_6\text{H}_6$ . However, in the case of the ethylene<sup>[30]</sup> and methane<sup>[31]</sup> dimers it has been shown that the MP4 correction to the MP2 correlation energy is only of few percent. A high quality basis set is also required<sup>[30]</sup> when dealing with van der Waals interactions, and accordingly we used Dunning’s triple-zeta quality basis set cc-pVTZ.<sup>[32]</sup> The geometry of the monomers was optimized at the MP2/cc-pVTZ level, except for the benzene dimers **4a** and **4b**; here the experimental geometry was used. For each case we performed several calculations as a function of the

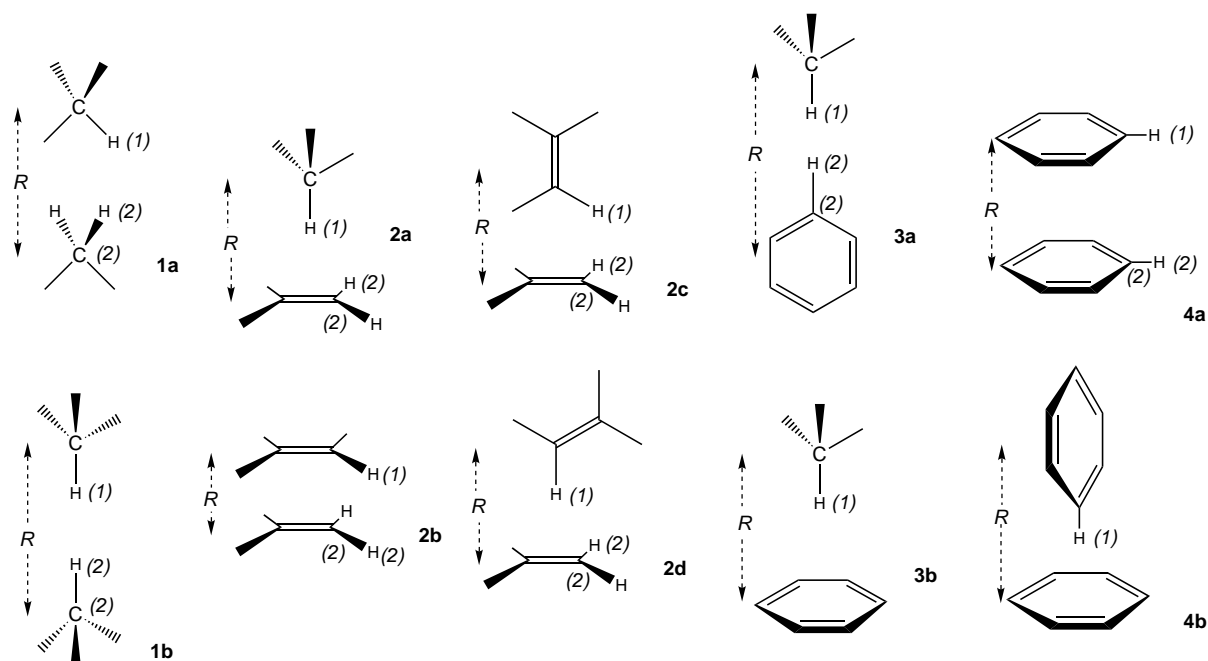


Figure 1. Schematic representation of the van der Waals dimers model systems.

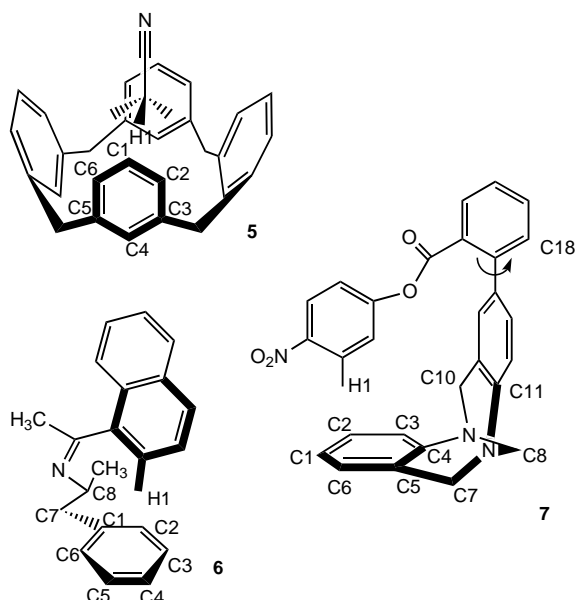


Figure 2. Schematic representation of the three CH/π interacting compounds investigated.

intermolecular separation with a step of 0.2 Å, at least around the minimum of the interaction energy.

**Ab initio calculations:** High-level ab initio methods like equation of motion-coupled cluster,<sup>[11–13]</sup> configuration interaction,<sup>[21a]</sup> multiconfiguration SCF<sup>[21b]</sup> and the second-order polarization propagator approximation (SOPPA)<sup>[33]</sup> have been used lately to calculate nuclear spin–spin couplings in covalent molecules as well as in hydrogen-bonded and van der Waals dimers. In particular, Pecul et al.<sup>[21b]</sup> carried on a detailed investigation of the dependence of the intermolecular  $J_{\text{HF}}$  coupling in  $\text{HF} \cdots \text{CH}_4$  on the basis set and size of the configurational space in Restricted Active Space Self-Consistent Field (RASSCF) calculations.

For the smaller dimers investigated here (**1** and **2**) we ran a series of calculations with the RASSCF method using a configuration space obtained by following the guidelines reported in ref. [21b]. Thus, we included in the active space all orbitals found to have an occupation number larger than 0.0043 at the MP2 level. For the  $\text{CH}_4 \cdots \text{CH}_4$  dimer, this implies that the two 1s orbitals of each methane molecule are inactive; the RAS1 space (holes) is empty, while the RAS2 and RAS3 active spaces contain eight and eighteen orbitals, respectively, and two electrons are excited into RAS3 space. The configuration space is then indicated as 2/0/8/18/2e. For the methane–ethylene dimer, the configuration space used was 3/0/10/21/2e, and for the ethylene–ethylene dimer 4/0/12/26/2e. The best compromise between accuracy and computational cost was obtained with Dunning's double-zeta basis set (cc-pVDZ) augmented with diffuse functions, fully decontracted *s* functions, and further augmented with one tight *s* function (aug-cc-pVDZ-*su1*).<sup>[21b]</sup> As a second test we also considered the SOPPA method with the same basis set. RASSCF and SOPPA calculations were run with the *Dalton 1.2* code,<sup>[34]</sup> which allows calculation of the four contributions to the spin–spin coupling: the Fermi Contact (FC), the Paramagnetic Spin–Orbit (PSO), the Diamagnetic Spin–Orbit (DSO) and the Spin–Dipole (SD) contributions. Thus,  $J = J^{\text{FC}} + J^{\text{PSO}} + J^{\text{DSO}} + J^{\text{SD}}$ . Its internal architecture does not allow 255 basis functions to be exceeded for such calculations; this renders it impossible to carry out any detailed analysis of basis-set effects in our systems (except perhaps for the methane dimer, which will be shown to behave differently from all others and therefore would not be a significant benchmark).

It is important to emphasize that the application of such high-level ab initio calculations is severely limited to small systems: it is extremely demanding even for the benzene dimers, and the large molecules **5–7** are absolutely intractable. DFT methods are then the only choice for the larger systems.

**DFT calculations:** DFT calculations were performed with the *deMon-NMR* code,<sup>[35]</sup> which allows the calculation of the three contributions to the

nuclear spin–spin coupling generally supposed to be of major importance, that is, FC, DSO, and PSO.

For the smallest system (the  $\text{CH}_4 \cdots \text{CH}_4$  dimer) we ran the calculations with two different functionals: the local Vosko–Wilk–Nusair exchange–correlation functional<sup>[36]</sup> (VWN) and the Perdew–Wang 1986 exchange<sup>[37]</sup> with Perdew 1986 correlation<sup>[38]</sup> (PWP). The PWP functional is strongly recommended for the calculation of spin–spin couplings; for  $^1J_{\text{CH}}$  in hydrocarbons (methane, ethylene, benzene) the calculated results are within a few percent of the experimental data.<sup>[35e]</sup> In the present case, presumably because the nuclei with which we are concerned are separated by a relatively large distance, we found that the two functionals gave almost identical results. Moreover, an EXTRAFINE grid (64 radial points) is required to have accurate results with the PWP functional, while the same accuracy is obtained with a FINE grid (32 radial points) for the VWN functional.<sup>[35e]</sup> this substantially reduces the running time. For this reason we only used the VWN functional for the larger dimers with ethylene and benzene, and for the CH/π examples **5**, **6**, and **7**. The perturbation parameter  $\lambda$  was set to 0.001 and placed on the lighter atom.<sup>[35e]</sup> The basis set used for these calculations was IGLO-III by Kutzelnigg et al.<sup>[39]</sup> In the *deMon* implementation, this basis is the largest for which all fitting parameters have been determined.

## Results

**Methane dimers:** Two different geometries have been investigated: the crossed configuration **1a** and the linear one **1b** (Figure 1). Interaction energies are shown in Figure 3; the intermolecular distance *R* is measured between the centers of symmetry of the two monomers. The interaction energy of **1a** (Figure 3a) shows a shallow minimum for  $R = 4.200$  Å, corresponding to a stabilization of 0.24 kcal mol<sup>−1</sup>, whereas for the linear configuration **1b** (Figure 3b) the stabilization energy is smaller (only 0.11 kcal mol<sup>−1</sup>), and the minimum occurs at  $R = 4.971$  Å.

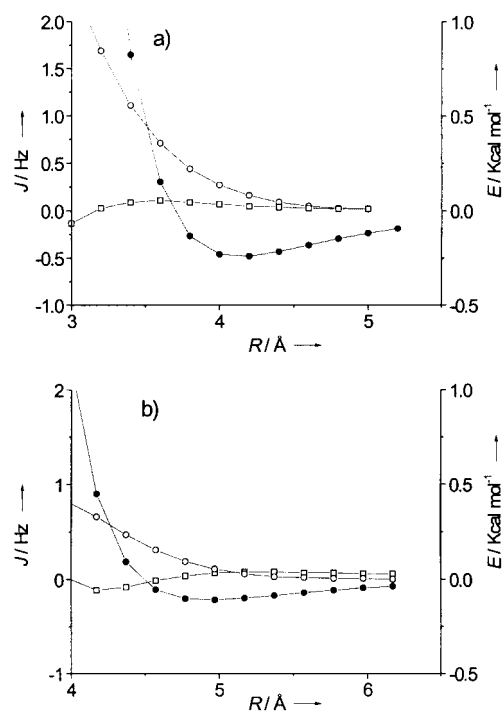


Figure 3. Interaction energy *E* and nuclear spin–spin coupling constants *J* for the methane dimers **1a** (a) and **1b** (b). BSSE-corrected MP2/cc-pVTZ interaction energies (●, right axis);  $J_{\text{HH}}$  (□) and  $J_{\text{CH}}$  (○) (left axis) at the VWN/IGLO-III level.

The  $J_{\text{HH}}$  and  $J_{\text{CH}}$  intermolecular couplings were calculated between the hydrogen labeled in Figure 1 as (1) on one molecule and the hydrogen or carbon nucleus on the other molecule, labeled as (2). For the dimer **1a** all three theoretical methods have been used to calculate the intermolecular  $J_{\text{CH}}$  and  $J_{\text{HH}}$  couplings, and the results are reported in Table 1 for some distances around the equilibrium geometry.

The SD term is smaller (almost by one order of magnitude) than the other contributions, but not negligible, at least at short distances. All the three methods yield the same value for  $J^{\text{DSO}}$ , which does not depend on correlation effects,<sup>[40]</sup> but DFT yields a larger  $J^{\text{PSO}}$  than RASSCF and SOPPA.

We remark that  $J^{\text{PSO}} + J^{\text{DSO}} + J^{\text{SD}}$  at the RASSCF and SOPPA levels is essentially zero, as is  $J^{\text{PSO}} + J^{\text{DSO}}$  at the DFT level. In contrast,  $J^{\text{FC}}$  is by far the largest contribution and accordingly dominates the total coupling. The FC contribution calculated by DFT is substantially larger than the values obtained by RASSCF and SOPPA, which are in very good agreement with one another. Thus, DFT systematically predicts  $J_{\text{CH}}$  to be 1.5 times larger than what is predicted by RASSCF and SOPPA, despite the high accuracy of DFT in calculating spin–spin couplings in covalent hydrocarbons.<sup>[35e]</sup>

The calculations at other distances for dimer **1a**, and all calculations for **1b**, were run only at the DFT level (Figure 3). In the range of intermolecular separations where the interaction is stabilizing,  $J_{\text{HH}}$  is negligible. The DSO and PSO contributions to  $J_{\text{HH}}$  almost exactly cancel each other, even though they can be significantly larger than the FC term, as observed in covalent molecules.<sup>[41]</sup>

Analogous results are obtained for the linear configuration **1b** (Figure 3b and Table 3, below). The  $J_{\text{HH}}$  values are again almost negligible in the stabilizing region, while  $J_{\text{CH}}$  values can reach about 0.3 Hz at a distance of 4.6 Å, but are extremely small at the equilibrium distance.

**Methane–ethylene and ethylene–ethylene dimers:** Dimer **2a**, in which an alkyl residue interacts with an unsaturated carbon, provides a prototype CH/ $\pi$  interaction. Interaction energies are given in Figure 4; for  $R = 4.285$  Å, we have a stabilization energy of 0.41 kcal mol<sup>−1</sup>.

For this system, we calculated the  $J_{\text{CH}}$  intermolecular couplings between hydrogen (1) of methane and the two equivalent carbons (2) of ethylene (Figure 1) at the SOPPA and DFT levels. In Table 2 we show the results for some distances around the equilibrium separation, plus the RASSCF result at the equilibrium distance.

Several differences appear between **2a** and **1a**. By DFT,  $J^{\text{FC}}$  is still significantly larger than by ab initio, but very small.

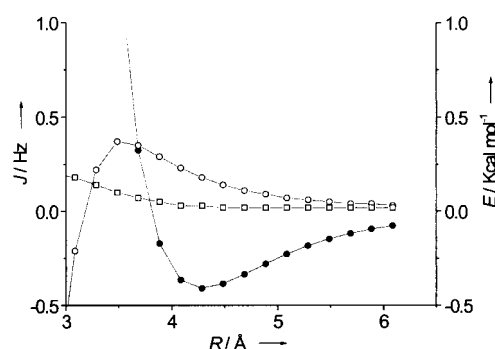


Figure 4. Interaction energy  $E$  and nuclear spin–spin coupling constants  $J$  for the methane–ethylene dimer **2a**. BSSE-corrected MP2/cc-pVTZ interaction energies (●, right axis);  $J_{\text{HH}}$  (□) and  $J_{\text{CH}}$  (○) (left axis) at the VWN/IGLO-III level.

According to SOPPA or RASSCF results,  $J^{\text{FC}}$  is smaller than  $J^{\text{SD}}$  (which, unlike for **1a**, is positive). On the other hand, spin–orbit terms do not cancel each other out as in the case of the dimer **1a**:  $J^{\text{PSO}} + J^{\text{DSO}} + J^{\text{SD}}$  at the SOPPA level, and  $J^{\text{PSO}} + J^{\text{DSO}}$  at the DFT level, are much larger than  $J^{\text{FC}}$ . Since, as noted before, the leading DSO term is calculated accurately also by DFT, it turns out that the disagreement between DFT and ab initio calculations, in this case, is smaller than for **1a**. More interestingly from the perspective on an experimental verification, it appears that DFT underestimates  $J_{\text{CH}}$  with respect to the ab initio results, at least for separations around the equilibrium. We again note the quantitative agreement between the SOPPA and RASSCF methods as seen for **1a**. Some more distances and the  $J_{\text{HH}}$  couplings have been investigated at the DFT level (Figure 4). Once again  $J_{\text{HH}}$  is almost negligible, whilst a value of 0.18 Hz is calculated for  $J_{\text{CH}}$  at the equilibrium separation. We have also calculated the  $J_{\text{HH}}$  coupling at the SOPPA level for the equilibrium distance of the dimer **2a**. In agreement with the DFT result, the FC and SD terms are almost negligible. However,  $J^{\text{PSO}}$  and  $J^{\text{DSO}}$ , at the SOPPA level, do not cancel each other exactly, as calculated at the DFT level; this produces a total coupling of 0.14 Hz. However, since the  $^{13}\text{C}, ^1\text{H}$  intermolecular coupling appears to be stronger, we did not further investigate the  $^1\text{H}, ^1\text{H}$  coupling with ab initio calculations for all the other systems.

We have also investigated the intermolecular couplings between alkenes, like the ethylene–ethylene dimers in the parallel configuration **2b** and the T configuration **2c**. For the parallel dimer **2b** we calculate no stabilization<sup>[30]</sup> (Figure 5a), whereas for the T-shaped dimer **2c** the interaction energy (Figure 5b) shows a well-defined minimum (0.52 kcal mol<sup>−1</sup> at  $R = 4.6$  Å).<sup>[30]</sup>

Table 1. Comparison of ab initio and DFT methods for the  $J_{\text{CH}}$  intermolecular spin–spin coupling (Hz) in the methane dimer **1a** at some intermolecular separations ( $R_{\text{eq}} = 4.2$  Å).

	3.6 Å			3.8 Å			4.0 Å			4.2 Å		
	DFT <sup>[a]</sup>	SOPPA <sup>[b]</sup>	RAS <sup>[c]</sup>	DFT <sup>[a]</sup>	SOPPA <sup>[b]</sup>	RAS <sup>[c]</sup>	DFT <sup>[a]</sup>	SOPPA <sup>[b]</sup>	RAS <sup>[c]</sup>	DFT <sup>[a]</sup>	SOPPA <sup>[b]</sup>	RAS <sup>[c]</sup>
DSO	0.15	0.15	0.15	0.13	0.13	0.13	0.12	0.11	0.12	0.11	0.10	0.11
PSO	−0.14	−0.11	−0.11	−0.13	−0.10	−0.10	−0.11	−0.09	−0.09	−0.10	−0.08	−0.08
SD	−	−0.04	−0.04	−	−0.03	−0.03	−	−0.02	−0.02	−	−0.02	−0.02
FC	0.71	0.50	0.48	0.44	0.31	0.29	0.26	0.18	0.17	0.15	0.10	0.09
TOT	0.72	0.50	0.48	0.44	0.31	0.29	0.27	0.18	0.18	0.16	0.10	0.10

[a] DFT-VWN/IGLO-III. [b] SOPPA/aug-cc-pVDZ-su1. [c] RASSCF-(2/0/8/18/2e)/aug-cc-pVDZ-su1.

Table 2. Comparison of ab initio and DFT methods for the  $J_{\text{CH}}$  intermolecular spin–spin coupling (Hz) in the methane–ethylene dimers **2a,c,d** at some intermolecular separations.

Contribution	DFT <sup>[a]</sup>	SOPPA <sup>[b]</sup>	RAS <sup>[c]</sup>
<b>2a</b> , 3.685 Å			
DSO	0.38	0.38	
PSO	−0.23	−0.15	
SD	–	0.08	
FC	0.20	−0.02	
Total	0.35	0.29	
<b>2a</b> , 3.885 Å			
DSO	0.33	0.33	
PSO	−0.20	−0.13	
SD	–	0.06	
FC	0.16	0.03	
Total	0.29	0.29	
<b>2a</b> , 4.085 Å			
DSO	0.29	0.29	
PSO	−0.18	−0.12	
SD	–	0.05	
FC	0.11	0.04	
Total	0.23	0.26	
<b>2a</b> , 4.285 Å <sup>[d]</sup>			
DSO	0.26	0.26	0.26
PSO	−0.16	−0.11	−0.11
SD	–	0.04	0.04
FC	0.07	0.03	0.02
Total	0.18	0.22	0.21
<b>2a</b> , 4.485 Å			
DSO	0.23	0.23	
PSO	−0.14	−0.10	
SD	–	0.03	
FC	0.05	0.02	
Total	0.14	0.18	
<b>2c</b> , 4.600 Å <sup>[d]</sup>			
DSO	0.23	0.23	
PSO	−0.13	−0.09	
SD	–	−0.07	
FC	0.09	0.05	
Total	0.19	0.12	
<b>2d</b> , 4.280 Å <sup>[e]</sup>			
DSO	0.28	0.28	0.28
PSO	−0.18	−0.12	−0.12
SD	–	0.04	0.04
FC	0.06	0.02	0.00
Total	0.16	0.22	0.20

[a] DFT-VWN/IGLO-III. [b] SOPPA/aug-cc-pVDZ-su1. [c] RASSCF-(3/0/10/21/2e)/aug-cc-pVDZ-su1. [d] Equilibrium distance. [e] Distance between the carbon atom to which H-1 is bonded and center of symmetry of ethylene molecule (2) (see Figure 1).

Both  $J_{\text{HH}}$  and  $J_{\text{CH}}$ , at the DFT level, are almost zero in the case of **2b** (Figure 5a). For **2c**,  $J_{\text{HH}}$  is again negligible, but  $J_{\text{CH}}$  is about 0.2 Hz at the equilibrium distance. As we can see in Table 3, there is an almost exact compensation between the DSO and PSO contributions for  $J_{\text{HH}}$ , while a relatively large contribution from spin–orbit terms can be observed in  $J_{\text{CH}}$ . For **2c** we also calculated the  $J_{\text{CH}}$  coupling with the SOPPA method at  $R_{\text{eq}} = 4.6$  Å (Table 2).  $J^{\text{DSO}}$  is exactly the same as obtained by DFT, whereas  $J^{\text{PSO}}$  and  $J^{\text{FC}}$  are larger at the DFT level than the corresponding ab initio values. Moreover, the ab initio results show that the magnitude of  $J^{\text{SD}}$  is larger than that of  $J^{\text{FC}}$ , but with a negative sign. These results add up to a total coupling of 0.12 Hz, to be compared with the DFT result of 0.19 Hz, in which the SD term was neglected. Again, the DFT result is larger than the ab initio results as found for **1a**.

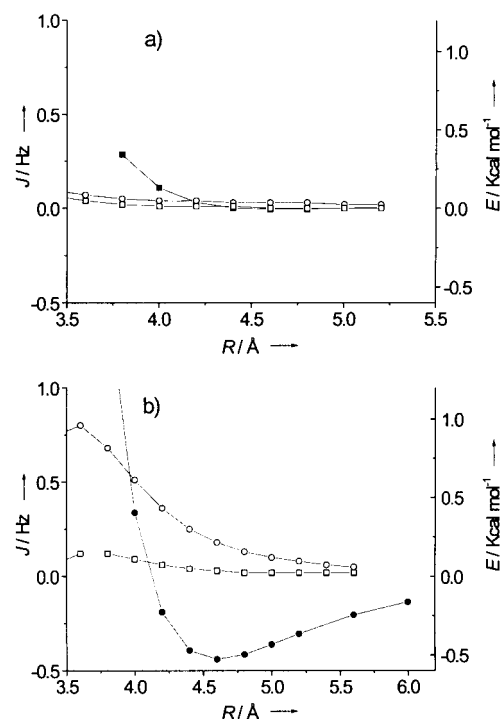


Figure 5. Interaction energy  $E$  and nuclear spin–spin coupling constants  $J$  for the ethylene dimers **2b** (a) and **2c** (b). BSSE-corrected MP2/cc-pVTZ interaction energies (●, right axis);  $J_{\text{HH}}$  (□) and  $J_{\text{CH}}$  (○) (left axis) at the VWN/IGLO-III level.

Table 3. Intermolecular spin–spin couplings calculated by DFT at selected distances.<sup>[a]</sup>

Dimer	$R$ <sup>[b]</sup>	$J_{\text{HH}}$			$J_{\text{CH}}$		
		FC	PSO	DSO	FC	PSO	DSO
<b>1a</b>	5.000	−0.01	−0.70	0.72	0.01	−0.07	0.08
	4.200	0.02	−0.99	1.02	0.15	−0.10	0.11
	3.600	0.07	−1.34	1.38	0.71	−0.14	0.15
<b>1b</b>	6.171	−0.01	−1.13	1.19	0.01	−0.10	0.10
	4.971	−0.06	−2.04	2.17	0.12	−0.16	0.15
	4.571	−0.17	−2.62	2.78	0.33	−0.20	0.18
<b>2c</b>	5.600	0.00	−0.41	0.43	0.00	−0.09	0.14
	4.600	0.01	−0.65	0.67	0.09	−0.13	0.23
	4.000	0.06	−0.90	0.93	0.35	−0.19	0.34
<b>3a</b>	6.485	−0.04	−2.18	2.29	0.09	−0.28	0.26
	6.085	−0.13	−2.74	2.88	0.27	−0.34	0.31
	5.685	−0.28	−3.57	3.75	0.59	−0.42	0.37
<b>3b</b>	4.485	0.00	−0.21	0.21	0.02	−0.19	0.26
	3.685	0.00	−0.13	0.12	0.11	−0.30	0.41
	3.285	0.01	−0.02	0.00	0.19	−0.42	0.53
<b>4a</b>	5.000	0.00	−0.39	0.39	0.00	−0.05	0.08
	3.800	−0.01	−0.75	0.76	0.01	−0.10	0.15
	3.300	0.15	−1.14	1.14	0.12	−0.13	0.21
<b>4b</b>	5.100	0.00	−0.33	0.32	0.08	−0.36	0.46
	4.900	0.00	−0.30	0.28	0.11	−0.42	0.52
	4.400	0.04	−0.16	0.13	0.07	−0.64	0.73

[a] In hertz at the VWN/IGLO-III level. See Table 2 for data of **2a** and **2d**; couplings for **2b** are always negligible (see text). [b] In Å (see Figure 1).

Since our interest lies mainly with CH/ $\pi$  interacting compounds, we also calculated  $J_{\text{CH}}$  for the ethylene dimer **2d**, obtained from **2c** by rotating the top ethylene molecule by 60° in the same plane, so that a C–H bond pointed perpendicularly toward the C=C double bond of the bottom

ethylene molecule (Figure 1). The distance between the C=C midpoint and the hydrogen of the C–H bond was set to 3.2 Å, corresponding to the equilibrium separation of **2a**. The different orientation of the C–H bond changes the sign of  $J^{\text{SD}}$ , which becomes positive as calculated for **2a**. SOPPA and RASSCF yield essentially the same results (total 0.22–0.20 Hz), whereas DFT gives a total of 0.16 Hz, the positive SD contribution being neglected. Therefore, when the C–H bond is perpendicular to the  $\pi$  system, DFT underestimates the ab initio results as was the case for the methane–ethylene dimer **2a**, to which it is geometrically related.

**Arene dimers:** As an example of an alkyl–aromatic interaction, we considered the  $\text{CH}_4 \cdots \text{C}_6\text{H}_6$  dimer in two different configurations, that is, linear (**3a**) and T-shaped (**3b**). For **3a**, the interaction energy shows a shallow minimum at  $R = 6.085$  Å (Figure 6a), with a weak stabilization of  $0.18 \text{ kcal mol}^{-1}$ ; this is consistent with the large distance that the methane molecule necessarily has from the  $\pi$  system of benzene. At the DFT level,  $J_{\text{HH}}$  is again almost negligible in the range of distances in which the dimer is not destabilized, but  $J_{\text{CH}}$  is about 0.2 Hz at the equilibrium separation.

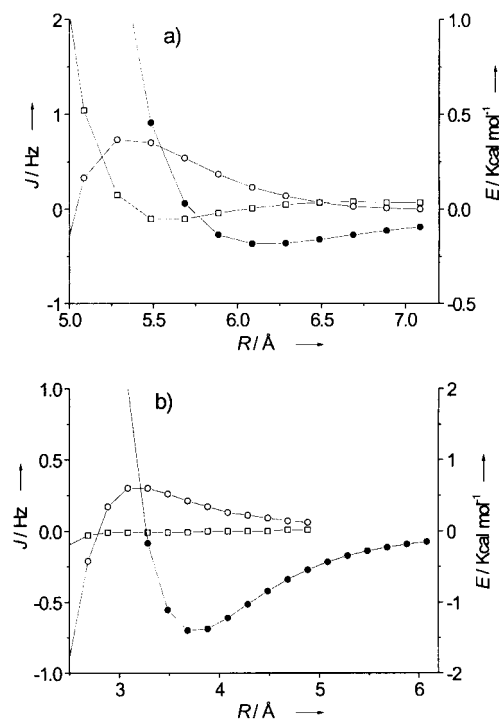


Figure 6. Interaction energy  $E$  and nuclear spin–spin coupling constants  $J$  for the methane–benzene dimers **3a** (a) and **3b** (b). BSSE-corrected MP2/cc-pVTZ interaction energies (●, right axis);  $J_{\text{HH}}$  (□) and  $J_{\text{CH}}$  (○) (left axis) at the VWN/IGLO-III level.

In Figure 6b we report the results for the  $\text{CH}_4 \cdots \text{C}_6\text{H}_6$  dimer in the T-shaped configuration **3b**. The interaction energy has a relatively deep minimum (a stabilization energy of  $1.40 \text{ kcal mol}^{-1}$ ) for  $R = 3.685$  Å.  $J_{\text{HH}}$  is again essentially zero throughout the distances investigated, while  $J_{\text{CH}}$  is noticeable (0.2 Hz at equilibrium distance). From Table 3 we again observe that for  $J_{\text{HH}}$ ,  $J^{\text{PSO}}$  and  $J^{\text{DSO}}$  are larger than  $J^{\text{FC}}$ , but

that they cancel each other to a large extent. For  $J_{\text{CH}}$  the contribution from spin–orbit terms is significant, instead.

Finally, we investigated two benzene molecules in the parallel (**4a**) and T-shaped (**4b**) configurations. These calculations were done with the monomer having the experimental geometry<sup>[42]</sup> (tests employing MP2/cc-pVTZ geometries led to the same results). In Figure 7a we show the interaction energy and couplings for the parallel configuration **4a**. The energy minimum ( $2.50 \text{ kcal mol}^{-1}$ ) occurs at  $R = 3.80$  Å.<sup>[30, 43]</sup> The coupling appears to be weak at the equilibrium separation, although a detectable coupling is observable before the two molecules start to overlap.

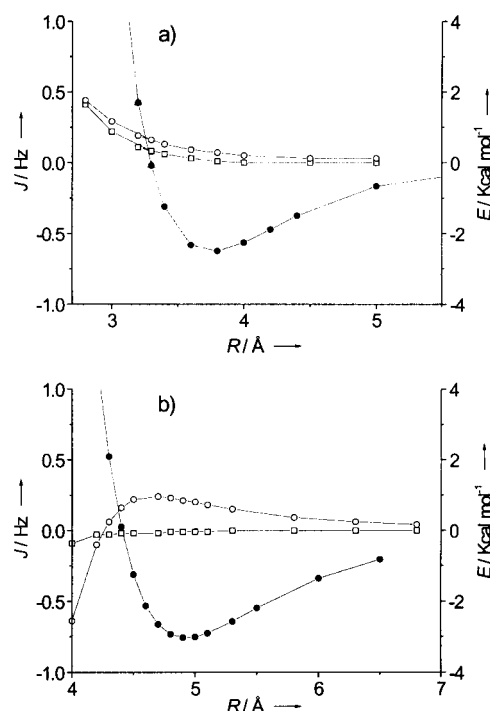


Figure 7. Interaction energy  $E$  and nuclear spin–spin coupling constants  $J$  for the benzene dimers **4a** (a) and **4b** (b). BSSE-corrected MP2/cc-pVTZ interaction energies (●, right axis);  $J_{\text{HH}}$  (□) and  $J_{\text{CH}}$  (○) (left axis) at the VWN/IGLO-III level.

Interaction energies and couplings for the benzene dimer in the T-shaped configuration **4b** are reported in Figure 7b. The stabilization energy is relatively large ( $3.02 \text{ kcal mol}^{-1}$ ,  $R = 4.90$  Å).<sup>[30, 43]</sup> As in the previous cases,  $J_{\text{HH}}$  is almost zero, whereas  $J_{\text{CH}} = 0.21 \text{ Hz}$  at the equilibrium distance. Once again, a significant contribution to  $J_{\text{CH}}$  comes from the incomplete compensation of the PSO and DSO terms (see Table 3).

**CH/ $\pi$  interacting systems:** The calculations on the large compounds **5**, **6**, and **7** were run only by DFT at the VWN/IGLO-III level. The X-ray structure of the inclusion compound acetonitrile@calix[4]arene, **5**,<sup>[44]</sup> shows that the guest molecule enters the cavity of the calixarene with the methyl group first, its C–H bonds roughly pointing toward the benzene rings of the host. The local arrangement of the C–H/benzene group is, then, very similar to the model **3b**. The distance between the methyl carbon and the center of

symmetry of one of the aromatic rings is found to be 3.71 Å. This is very close to the distance corresponding to the minimum of the interaction energy in Figure 6b, and confirms the importance of dispersive interactions in the stabilization of this kind of complexes. To reduce the computational effort, the *tert*-butyl and hydroxyl groups of the original calix[4]arene were replaced by hydrogen atoms. All hydrogen atoms (not observed by X-ray), were then quickly optimized at the PM3 semiempirical level, keeping all other atomic coordinates fixed. Finally, the perturbation was placed on the hydrogen labeled H1 in **5**. The results are reported in Table 4, and are fully consistent with those obtained for the model system **3b**.

Table 4. Intermolecular  $J_{\text{CH}}$  spin–spin couplings for the three CH/ $\pi$  interacting compounds.<sup>[a]</sup>

	5	6	7
C1	0.09	0.16	0.30
C2	0.11	0.13	0.25
C3	0.13	0.17	0.09
C4	0.19	0.18	0.01
C5	0.13	0.22	0.08
C6	0.12	0.16	0.24

[a] In hertz at the VWN/IGLO-III level, between the hydrogen H1 and the carbon atoms of the benzene ring facing the CH bond. [b] See Figure 2.

The imine **6** also offers an example of a system, in which a hydrogen, in this case belonging to an aromatic C–H bond, is found to be quite close to a second benzene ring. Hamor et al.<sup>[45]</sup> found that the *E/Z* exchange by rotation about the imino bond is slow on the NMR time scale. The most abundant *Z* isomer has been isolated, and the X-ray structure reveals that the hydrogen atom H1 is only 2.7 Å above the face of the phenyl ring C1–C6. These observations make **6** a possible candidate for an experimental verification of the theoretical results presented in this work. We therefore calculated  $J_{\text{CH}}$  between H1 in **6** and the C1–C6 carbon atoms of the aromatic ring (Table 4).

Finally, we turn our attention to compound **7**. Wilcox and co-workers<sup>[47]</sup> found that this aryl ester exists as two conformers, the folded one in Figure 2 and an extended one, which can be obtained by a 180° rotation about the bond indicated. This process is slow on the NMR time scale, so two separate sets of signals can be detected. Compound **7** is another typical example of a CH/ $\pi$  interacting system, since the arrangement of the two interacting benzene moieties, determined by X-ray,<sup>[47]</sup> is almost exactly T-shaped with a distance of 4.95 Å between the two ring centers (i.e., essentially the same as the equilibrium distance of **4b**). However, the two benzene rings are arranged in a slightly different way than in **4b**, because the distance between H1 and C1 is only 2.72 Å, H1 being placed essentially above C1. Therefore we expect  $J_{\text{C1-H1}}$  to be larger than the couplings with the other carbon atoms of the phenyl ring. We also note that the two interacting atoms are separated by no less than 16 covalent bonds; this should reduce any through-bond coupling to zero. In order to reduce the size of the molecule without losing significant structural aspects, we replaced the methyl groups originally on C1 and C18 with hydrogen atoms. The results of such calculations are reported in Table 4.

Figure 8 reports the  $J$  values between H1 and the carbon atoms as a function of the number of connecting bonds for both the folded and the extended conformer.

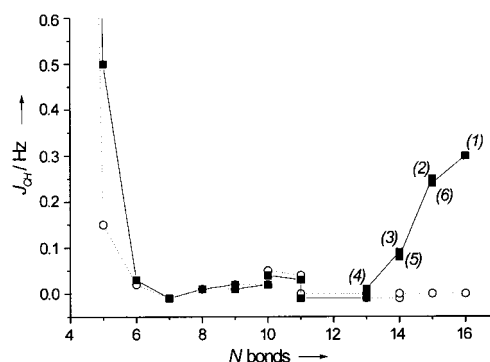


Figure 8.  $J_{\text{CH}}$  couplings, at the DFT-VWN/IGLO-III level, between hydrogen H1 and the carbon atoms of the aryl ester **7** as a function of the number  $N$  of connecting bonds. The carbon atoms of the benzene ring facing the C–H bond are labeled as in Figure 2. Folded conformer (■), extended conformer (○).

## Discussion

**General features—Ab initio versus DFT methods:** When dealing with dispersion-bound complexes, a point that arises naturally and needs to be addressed is whether DFT is at all adequate for the calculation of intermolecular couplings, given its notorious inability to deal with their energetics. This is a particularly sensitive point, since as yet there are no experimental data to provide an anchor. A straightforward way to work around this would be, of course, to adopt ab initio correlated methods, which are known to correctly predict the energetics. A strong point against this solution, however, lies in the extremely steep rise in the computational demands that follow even a modest increase in the size of the molecules involved, a necessary step to approach systems amenable to experimental studies. Thus, since even model complexes involving benzene are intractable, it is practically impossible to investigate large complexes like **5–7** by ab initio methods, even adopting a locally dense basis set;<sup>[33b]</sup> whereas they are quite within the scope of DFT. The solution we have adopted is to test the performance of two high-level ab initio methods (RASSCF and SOPPA) against DFT for simple models (the methane–methane and methane–ethylene dimers **1** and **2**), in order to establish at least some general trends. It is especially hoped that the latter will provide a model of the CH/ $\pi$  interaction.

We first note the essentially identical performance of SOPPA and RASSCF with the active space chosen. DFT and ab initio methods display somewhat different results; thus, for **2a** and **2d**, DFT couplings are smaller than ab initio by a factor of 0.8, and the reverse is true (by a factor of 1.6) for **1a** and **2c**, that is, the difference is not systematic. Part of the disagreement stems from the neglect of the SD term in DFT calculations; it is otherwise difficult to attribute these differences to some specific factor, such as the absence of tight *s* functions or diffuse functions in the basis sets used, or to the different treatment of correlation effects specific to each

method, or even to some fortuitous cancellation of errors. Even taking this uncertainty into account, the predicted values would still lie within the scope of high-level NMR experiments, and the favorable scaling of DFT methods allows large systems outside the scope of ab initio ones to be investigated (for such systems, in fact, DFT seems to *underestimate* the couplings with respect to ab initio, as noted above).

**Model Dimers:** Intermolecular spin–spin coupling between  $^1\text{H}$  and  $^{13}\text{C}$  in most van der Waals dimers is calculated to be not negligible, especially for systems in which a C–H bond is pointing toward a  $\pi$  system, as in the case of **2a**, **2c**, **2d**, **3b**, and **4b**. Some trends (relative contribution of contact and spin–orbit terms) seem to conform to the behavior of couplings in covalent molecules,<sup>[41]</sup> and absolute  $J_{\text{CH}}$  values may reach 0.2–0.3 Hz for geometrical arrangements close to the equilibrium distance. However, the predicted values are derived from a delicate balance among several very small terms; as a consequence, the spin–dipole term (usually considered to be negligible even in other van der Waals complexes<sup>[21b]</sup>) may play a decisive role in determining the total coupling, even though its value does not exceed 0.04 Hz in stabilizing regions.

The main factor involved in determining the magnitude of such couplings seems to be the internuclear distance. Thus, for the parallel dimers **4a** and, especially, **2b**, the negligible couplings arise simply from the larger C...H distance, compared with the analogous T-shaped dimers. However, the results for **2c** and **2d** (which differ only in the relative arrangement of monomers) suggest some angular dependence,<sup>[21b]</sup> especially of the SD term. On the other hand, the very similar results obtained for **2a** (at 4.285 Å) and **2d**, which differ only in the nature of the “donor” C–H bond (alkane or alkene), indicate that intermolecular coupling in CH/ $\pi$  systems may be independent of the nature of the involved partners.

It is also worth mentioning a characteristic dependence of  $J_{\text{CH}}$  on the intermolecular separation, which shows a change of sign after reaching a maximum at about the contact distance of the monomers (see for example Figures 4, 6b and 7b). The same behavior was predicted theoretically<sup>[20]</sup> for  $J_{^{129}\text{Xe},^{131}\text{Xe}}$  and experimentally found<sup>[6]</sup> for  $J_{\text{FH}}$  in FHF<sup>−</sup>, F(HF)<sub>2</sub><sup>−</sup>, F(HF)<sub>3</sub><sup>−</sup>, and F(HF)<sub>4</sub><sup>−</sup> HB complexes. Owing to the different geometry of such complexes, they could determine the coupling constant as a function of the F...HF distance.<sup>[6]</sup> Despite the difference in the absolute values ( $J_{\text{FH}}$  being larger by several orders of magnitude), the  $J_{\text{CH}}$  couplings calculated here show the same qualitative behavior.

**Intermolecular coupling for other nuclei and systems:** As mentioned earlier,  $^1\text{H}, ^1\text{H}$  couplings (<0.1 Hz) are generally much smaller than  $^1\text{H}, ^{13}\text{C}$ . In order to clarify their relative magnitude, we have to compare the reduced coupling constants

$$K_{\text{MN}} = \frac{J_{\text{MN}}}{h} \frac{2\pi}{\gamma_{\text{M}} \gamma_{\text{N}}}$$

which are independent of the magnetogyric ratios. Thus, a  $J_{\text{HH}}$  of 0.1 Hz corresponds to  $K_{^1\text{H},^1\text{H}} = 0.0083 \times 10^{19} \text{ T}^2 \text{ J}^{-1}$ , whereas assuming a  $J_{\text{CH}}$  value of 0.3 Hz, as in the aryl ester **7**, one obtains  $K_{^{13}\text{C},^1\text{H}} = 0.10 \times 10^{19} \text{ T}^2 \text{ J}^{-1}$ ; this illustrates the intrinsically stronger coupling in the latter case. Further comparisons can be made with He...He<sup>[21a]</sup> yielding  $K_{^3\text{He},^3\text{He}} = 0.19 \times 10^{19} \text{ T}^2 \text{ J}^{-1}$ , and with HF...CH<sub>4</sub>,<sup>[21b]</sup> for which  $K_{^1\text{H},^{19}\text{F}}$  is about  $0.4 \times 10^{19} \text{ T}^2 \text{ J}^{-1}$ , depending on the hydrogen considered. Hence, although there are individual variations, all reduced couplings fall within a similar range.

Hence, these weak couplings appear to be ubiquitous, since all current theoretical models predict a non-negligible magnitude for virtually every intermolecular arrangement, even those leading to extremely weak interactions (e.g. He...He). However, interestingly, no couplings are predicted for a non-interacting system like the planar ethylene dimer **2b**, and we also recall the angular dependence noted before. Other than this, there seems to be little if any indication that the existence of such couplings can be related per se to the strength of such “bonding”.<sup>[21a]</sup> We note in passing that test calculations on molecules substituted in ways that are expected to entail a stronger interaction (e.g. 1,3,5-trihydroxybenzene; data not reported) actually yield the same or even smaller couplings. These preliminary results point out that such substitutions do affect MO's in the  $\pi$  system, but have no effect on those that actually transmit the coupling, which are of  $\sigma$  symmetry.<sup>[27]</sup> This is somewhat analogous (with all due caveats) to hydrogen bonding, in which the symmetry of the occupied MO's connecting donor and acceptor could be related to the structural dependence of  $^{15}\text{N}-\text{H} \cdots \text{O}=\text{C}^{13}\text{C}$  coupling constants.<sup>[15]</sup>

We can then endorse Pecul's concept that through-space couplings are “a much more common phenomenon than previously thought”.<sup>[21a]</sup> However, owing to their nonspecific nature, their usefulness will be restricted to probing the spacial proximity of specific atoms, rather than the energetics of such interactions.

**CH/ $\pi$  complexes:** Intermolecular  $J_{\text{CH}}$  couplings in **5** range between 0.09 and 0.19 Hz, depending on the carbon atom of the benzene ring, as the structure is not perfectly symmetric. Since there is no covalent bond between host and guest, the non-negligible  $J_{\text{CH}}$  coupling we calculate must occur through space. However, we note that its measurement may be severely hampered by the mobile arrangement of the methyl group inside the cavity, which also depends on the temperature.

The analogous results for **6** are again fully consistent with the data obtained for the corresponding model dimer **4b**,  $J_{\text{CH}}$  being between 0.13 and 0.22 Hz. We note that the number of covalent bonds separating the atoms involved in the coupling is large, namely 7 for  $J_{\text{Cl-H1}}$  and up to 10 for  $J_{\text{C4-H1}}$ , and that the larger couplings are those involving atoms separated by the highest number of bonds; therefore the coupling must occur through space as in **5**. Moreover, couplings with the other carbon atoms in the chain (C7 and C8) are as small as −0.03 and 0.11 Hz, respectively. Therefore, the spin–spin couplings with the carbon atoms of the benzene ring are significantly higher than would be expected if only the number of bonds



separating the two interacting atoms were considered. Once again, however, one may expect great difficulties in the experimental verification, since a relatively strong temperature dependence of the chemical shift of H1 was observed and interpreted by assuming a fast conformational equilibrium with a species less sterically congested than structure **6**. Therefore, only at low temperature is conformer **6** expected to be the sole species present in solution.<sup>[46]</sup>

For **7**, as expected, intermolecular coupling is also significant, with  $J_{\text{C1-H1}} = 0.30$  Hz. The almost negligible value of  $J_{\text{C4-H1}}$ , despite the fact that C4 also belongs to the  $\pi$  system, can be attributed to their larger separation (3.54 Å). Almost negligible  $J_{\text{CH}}$  couplings, between  $-0.01$  and  $0.03$  Hz, are also obtained between H1 and C7–C10, even though there are fewer connecting bonds. This effect is highlighted in Figure 8: for the folded conformer, the couplings rapidly fall to negligible values after a few bonds, then rise up to a few tenths of hertz for the carbon atoms of the benzene ring facing the C–H bond. In contrast, for the extended conformer, where the C–H bond and the benzene ring are very far apart, the  $J_{\text{CH}}$  coupling with C1–C6 vanishes. Again, this clearly demonstrates that a through-space mechanism is operating.

We stress again that the CH/ $\pi$  interaction does not play any particular role other than stabilizing a structure in which a C–H bond is relatively close to a  $\pi$  system. This is evident from our last example, in which the coupling is only relatively large with the carbon atoms of the phenyl ring, which are close enough to the C–H bond. Therefore, through-space spin–spin coupling is not, in principle, a peculiar property of CH/ $\pi$  systems only, although it may be easier to observe in these compounds.

## Conclusion

We have investigated through-space spin–spin couplings in van der Waals dimers as models of molecules favorably arranged to exhibit the CH/ $\pi$  interaction. For the model systems, several computational methods, both ab initio and DFT, have been compared. All the results are rather similar considering the relatively small values involved; while  $^1\text{H}$ ,  $^1\text{H}$  couplings are generally very small or negligible, larger values (up to  $0.2$ – $0.3$  Hz) are predicted for  $^1\text{H}$ ,  $^{13}\text{C}$ .

In these compounds, DFT predicts coupling constants fully consistent with the results of the model systems. However, it has to be emphasized that typical van der Waals dimers such as **1**–**4** offer little if any prospect of an experimental validation. The situation appears to be much more favorable in the case of inclusion compounds like **5** and, especially, of conformationally restricted species, such as **6** and **7**. In these cases, in fact, it might be possible to observe such intermolecular couplings provided that the lifetime of the complex is long on the NMR timescale.

## Acknowledgement

We thank V. G. Malkin and O. L. Malkina for providing us with the *deMon-NMR* program. Part of this work was carried out through a generous grant of computer time on an SGI Origin 3800 at the CINECA supercomputer center.

- [1] See: G. Gemmecker, *Angew. Chem.* **2000**, *112*, 1276; *Angew. Chem. Int. Ed.* **2000**, *39*, 1224, and references therein for a brief summary of this field up to 1999.
- [2] F. Löhr, S. G. Mayhew, H. Rüterjans, *J. Am. Chem. Soc.* **2000**, *122*, 9289.
- [3] A. Liu, A. Majumdar, W. Hu, A. Kettani, E. Skripkin, D. J. Patel, *J. Am. Chem. Soc.* **2000**, *122*, 3206.
- [4] M. Mishima, M. Hatanaka, S. Yokoyama, T. Ikegami, M. Wächli, Y. Ito, M. Shirakawa, *J. Am. Chem. Soc.* **2000**, *122*, 5883.
- [5] J. E. Del Bene, S. A. Perera, R. J. Bartlett, I. Alkorta, J. Elguero, *J. Phys. Chem. A* **2000**, *104*, 7165.
- [6] I. G. Shenderovich, S. N. Smirnov, G. S. Denisov, V. A. Gindin, N. S. Golubev, A. Dunger, R. Reibke, S. Kirpekar, O. L. Malkina, H. H. Limbach, *Ber. Bunsen-Ges. Phys. Chem.* **1998**, *102*, 422.
- [7] M. Pecul, J. Sadlej, *Chem. Phys. Lett.* **1999**, *308*, 486.
- [8] A. J. Dingley, J. E. Masse, R. D. Peterson, M. Barfield, J. Feigon, S. Grzesiek, *J. Am. Chem. Soc.* **1999**, *121*, 6019.
- [9] M. Barfield, A. J. Dingley, J. Feigon, S. Grzesiek, *J. Am. Chem. Soc.* **2001**, *123*, 4014.
- [10] C. Scheurer, R. Brüschweiler, *J. Am. Chem. Soc.* **1999**, *121*, 8661.
- [11] J. E. Del Bene, S. A. Perera, R. J. Bartlett, *J. Phys. Chem. A* **1999**, *103*, 8121.
- [12] J. E. Del Bene, S. A. Perera, R. J. Bartlett, *J. Am. Chem. Soc.* **1999**, *121*, 3560.
- [13] J. E. Del Bene, M. J. T. Jordan, *J. Am. Chem. Soc.* **2000**, *122*, 4794.
- [14] a) M. Pecul, J. Leszczynski, J. Sadlej, *J. Phys. Chem. A* **2000**, *104*, 8105; b) M. Pecul, J. Leszczynski, J. Sadlej, *J. Chem. Phys.* **2000**, *112*, 7930.
- [15] A. Bagno, *Chem. Eur. J.* **2000**, *6*, 2925.
- [16] a) J. J. Dannenberg, L. Haskamp, A. Matsunov, *J. Phys. Chem. A* **1999**, *103*, 7083; b) A. Matsunov, J. J. Dannenberg, R. H. Contreras, *J. Phys. Chem. A* **2001**, *105*, 4737.
- [17] W. D. Arnold, E. Oldfield, *J. Am. Chem. Soc.* **2000**, *122*, 12835.
- [18] a) S. Jaime-Figueroa, L. J. Kurz, Y. Liu, R. Cruz, *Spectrochim. Acta* **2000**, *56A*, 1167; b) W. Adcock, M. Bullpitt, W. Kitching, *J. Org. Chem.* **1977**, *42*, 2411; c) G. W. Gribble, D. J. Keavy, E. R. Olson, I. D. Rae, A. Staffa, T. H. Herr, M. B. Ferraro, R. H. Contreras, *Magn. Reson. Chem.* **1991**, *29*, 422; d) F. B. Mallory, C. W. Mallory, K. E. Butler, M. B. Lewis, A. Q. Xia, E. D. Luzik, Jr., L. E. Fredenburgh, M. M. Ramanjulu, Q. N. Van, M. M. Francl, D. A. Freed, C. C. Wray, C. Hann, M. Nerz-Stormes, P. J. Carroll, L. E. Chirlian, *J. Am. Chem. Soc.* **2000**, *122*, 4108.
- [19] W. D. Arnold, J. Mao, H. Sun, E. Oldfield, *J. Am. Chem. Soc.* **2000**, *122*, 12164.
- [20] F. R. Salsbury, R. A. Harris, *Mol. Phys.* **1998**, *94*, 307.
- [21] a) M. Pecul, *J. Chem. Phys.* **2000**, *113*, 10835; b) M. Pecul, J. Sadlej, J. Leszczynski, *J. Chem. Phys.* **2001**, *115*, 5498.
- [22] a) M. Luhmer, B. M. Goodson, Y.-Q. Song, D. D. Laws, L. G. Kaiser, M. C. Cyrier, A. Pines, *J. Am. Chem. Soc.* **1999**, *121*, 3502; b) T. Brotin, T. Devic, A. Lesage, L. Emsley, A. Collet, *Chem. Eur. J.* **2001**, *7*, 1561.
- [23] M. Nishio, M. Hirota, Y. Umezawa, *The CH/ $\pi$  Interaction, Evidence, Nature and Consequences*, Wiley-VCH, New York, **1998**.
- [24] H. Takahashi, S. Tsuboyama, Y. Umezawa, K. Honda, M. Nishio, *Tetrahedron* **2000**, *56*, 6185.
- [25] F. H. Allen, J. E. Davies, J. J. Galloy, O. Johnson, O. Kennard, C. F. McRae, E. M. Mitchell, G. F. Mitchell, J. M. Smith, D. J. Watson, *J. Chem. Inf. Comput. Sci.* **1991**, *31*, 187.
- [26] O. W. Howarth, J. Nelson, V. McKee, *Chem. Commun.* **2000**, 21.
- [27] A. Bagno, G. Saielli, G. Scorrano, *Angew. Chem.* **2001**, *113*, 2600; *Angew. Chem. Int. Ed.* **2001**, *41*, 2532.
- [28] *Gaussian 98* (Revision A.7), M. J. Frisch, G. W. Trucks, H. B. Schlegel, G. E. Scuseria, M. A. Robb, J. R. Cheeseman, V. G. Zakrzewski, J. A. Montgomery, R. E. Stratmann, J. C. Burant, S. Dapprich, J. M. Millam, A. D. Daniels, K. N. Kudin, M. C. Strain, O. Farkas, J. Tomasi, V. Barone, M. Cossi, R. Cammi, B. Mennucci, C. Pomelli, C. Adamo, S. Clifford, J. Ochterski, G. A. Petersson, P. Y. Ayala, Q. Cui, K. Morokuma, D. K. Malick, A. D. Rabuck, K. Raghavachari, J. B. Foresman, J. Cioslowski, J. V. Ortiz, B. B. Stefanov, G. Liu, A. Liashenko, P. Piskorz, I. Komaromi, R. Gomperts, R. L. Martin, D. J. Fox, T. Keith, M. A. Al-Laham, C. Y. Peng, A. Nanayakkara, C. Gonzalez, M. Challacombe, P. M. W. Gill, B. G. Johnson, W. Chen, M. W. Wong, J. L. Andres, M. Head-Gordon, E. S. Replogle, J. A. Pople, Gaussian, Inc., Pittsburgh PA, **1998**.

- [29] S. F. Boys, F. Bernardi, *Mol. Phys.* **1970**, *19*, 553.
- [30] S. Tsuzuki, T. Uchimaru, M. Mikami, K. Tanabe, *Chem. Phys. Lett.* **1996**, *252*, 206.
- [31] S. Tsuzuki, K. Tanabe, *J. Phys. Chem.* **1991**, *95*, 2272.
- [32] T. H. Dunning, *J. Chem. Phys.* **1987**, *98*, 1007.
- [33] a) T. Enevoldsen, J. Oddershede, S. P. A. Sauer, *Theor. Chem. Acc.* **1998**, *100*, 275; b) P. F. Provasi, G. A. Aucar, S. P. A. Sauer, *J. Chem. Phys.* **2000**, *112*, 6201; c) P. F. Provasi, G. A. Aucar, S. P. A. Sauer, *J. Chem. Phys.* **2001**, *115*, 1324.
- [34] T. Helgaker, H. J. Aa. Jensen, P. Jørgensen, J. Olsen, K. Ruud, H. Ågren, A. A. Auer, K. L. Bak, V. Bakken, O. Christiansen, S. Coriani, P. Dahle, E. K. Dalskov, T. Enevoldsen, B. Fernandez, C. Hättig, K. Hald, A. Halkier, H. Heiberg, H. Hettema, D. Jonsson, S. Kirpekar, R. Kobayashi, H. Koch, K. V. Mikkelsen, P. Norman, M. J. Packer, T. B. Pedersen, T. A. Ruden, A. Sanchez, T. Saue, S. P. A. Sauer, B. Schimmelpfennig, K. O. Sylvester-Hvid, P. R. Taylor, O. Vahtras, *Dalton, a molecular electronic structure program*, Release 1.2, **2001**.
- [35] a) D. R. Salahub, R. Fournier, P. Mlynarski, I. Papai, A. St-Amant, J. Ushio in *Density Functional Methods in Chemistry* (Eds.: J. Labanowski, J. Andzelm), Springer, New York, **1991**; b) A. St-Amant, D. R. Salahub, *Chem. Phys. Lett.* **1990**, *169*, 387; c) V. G. Malkin, O. L. Malkina, M. Casida, D. R. Salahub, *J. Am. Chem. Soc.* **1994**, *116*, 5898; d) V. G. Malkin, O. L. Malkina, L. A. Eriksson, D. R. Salahub in *Modern Density Functional Theory: A Tool for Chemistry*, Vol. 2 (Eds.: J. M. Seminario, P. Politzer), Elsevier, Amsterdam, **1995**; e) V. G. Malkin, O. L. Malkina, D. R. Salahub, *Chem. Phys. Lett.* **1994**, *221*, 91; f) O. L. Malkina, D. R. Salahub, V. G. Malkin, *J. Chem. Phys.* **1996**, *105*, 8793.
- [36] S. H. Vosko, L. Wilk, M. Nusair, *Can. J. Phys.* **1980**, *58*, 1200.
- [37] J. P. Perdew, Y. Wang, *Phys. Rev. B* **1986**, *33*, 8800.
- [38] J. P. Perdew, *Phys. Rev. B* **1986**, *33*, 8822.
- [39] W. Kutzelnigg, U. Fleischer, M. Schindler, *NMR-Basic Principles and Progress*, Vol. 23, Springer, Berlin, **1990**.
- [40] T. Helgaker, M. Jaszunski, K. Ruud, *Chem. Rev.* **1999**, *99*, 293.
- [41] A. Bagno, *Chem. Eur. J.* **2001**, *7*, 1652.
- [42] *Handbook of Chemistry and Physics*, 69th ed., CRC Press, Boca Raton, **1988–1989**.
- [43] R. L. Jaffe, G. D. Smith, *J. Chem. Phys.* **1996**, *105*, 2780.
- [44] W. Xu, R. J. Puddephatt, L. Manojlovic-Muir, K. W. Muir, C. S. Frampton, *J. Incl. Phenom.* **1994**, *19*, 277.
- [45] T. A. Hamor, W. B. Jennings, L. D. Proctor, M. S. Tolley, D. R. Boyd, T. Mullan, *J. Chem. Soc. Perkin Trans. 2* **1990**, 25.
- [46] S. Paliwal, S. Geib, C. S. Wilcox, *J. Am. Chem. Soc.* **1994**, *116*, 4497.

Received: November 5, 2001 [F3660]